Microchemical Journal 224 (2026) 117446

Contents lists available at ScienceDirect

Microchemical Journal

journal homepage: www.elsevier.com/locate/microc

# In situ microRaman spectroscopy as a screening tool for assessing human DNA preservation in ancient dental remains

Aggelos Philippidis [a,*], Angeliki Mamali [a,h], Victor Pinon [a], Despoina Vassou [b], Argyro Nafplioti [b], Eugenia Tabakaki [b], Nikos Poulakakis [b,c,d], Alexandros Stamatakis [e,f,g], Pavlos Pavlidis [d,e], Nikolaos Psonis [b], Demetrios Anglos [a,h,*]

[a] Institute of Electronic Structure and Laser (IESL), Foundation for Research and Technology - Hellas (FORTH), GR70013 Heraklion, Crete, Greece
[b] Ancient DNA Lab, Institute of Molecular Biology and Biotechnology (IMBB), Foundation for Research and Technology - Hellas (FORTH), GR70013 Heraklion, Crete, Greece
[c] Natural History Museum of Crete (NHMC), School of Sciences and Engineering, University of Crete, GR71409 Heraklion, Crete, Greece
[d] Department of Biology, University of Crete, GR70013 Heraklion, Crete, Greece
[e] Institute of Computer Science (ICS), Foundation for Research and Technology-Hellas (FORTH), GR70013 Heraklion, Crete, Greece
[f] Heidelberg Institute for Theoretical Studies, Heidelberg, Germany
[g] Institute of Theoretical Informatics, Karlsruhe Institute of Technology, Karlsruhe, Germany
[h] Department of Chemistry, University of Crete, GR71003, Heraklion, Crete, Greece

ARTICLE INFO

Dataset link: raw Raman data (Original data)

*Keywords:*
Ancient teeth
Ancient DNA
Raman spectroscopy
Spectral indicators

ABSTRACT

Ancient DNA (aDNA) and protein analysis of human remains enables reconstructions of population history, kinship, diet, health and social structure of ancient communities. Ancient DNA yields important genetic information, nonetheless its extraction requires sampling, which is an important concern especially for rare and valuable samples. Furthermore, poor preservation of aDNA results to low endogenous DNA yield, and considering that analyses are costly and time-consuming, efficient pre-screening methods are needed to identify samples with higher probability of aDNA survival. Here, we present an in situ, non-invasive micro-Raman spectroscopy approach as a screening tool capable of predicting DNA preservation in ancient teeth. Because aDNA tends to persist in teeth preserving part of their proteinaceous (primarily collagen) component, the relative abundance of protein to mineral provides an indirect indication for DNA preservation. A set of 49 ancient teeth, dated from 8800 BCE to 1941 CE, were analyzed using for sample classification the amide-to-phosphate [AmI/P] index, defined as the intensity ratio of the amide I band (1666 $cm^{-1}$) over the phosphate band ($PO_4^{3-}$, 957 $cm^{-1}$). Measurements on the cementum area of the teeth, known to be protein-rich, revealed a weak but clear correlation between [AmI/P] and endogenous DNA amounts, independently determined via standard aDNA analysis. Among 25 aDNA-rich teeth, 23 were correctly identified (92% acceptance), and 13 of 20 aDNA-poor teeth were indicated to be so (65% rejection). Overall, Raman spectroscopy provides a valid, in situ, non-invasive pre-screening strategy for prioritizing ancient teeth with higher collagen content and greater likelihood of yielding endogenous human DNA.

## 1. Introduction

Ancient DNA (aDNA) analysis has become a transformative tool in archaeology, anthropology, and palaeogenomics, enabling direct insights into the genetic makeup, population history, genetic relationships, and even the health of past human populations [1–5]. Studying DNA sequences as well as proteins from ancient human or animal remains found in archaeological contexts, such as teeth and bones, can reveal the biological sex of individuals [6,7] and, in conjunction with complementary analysis of associated artifacts and burial practices, provide insights into kinship, as well as their social status within past societies [8]. In addition, polymorphism patterns in population-level samples allow researchers to infer past population size changes, admixture, migration (via gene flow), and genetic interactions among

* Corresponding authors at: Institute of Electronic Structure and Laser (IESL), Foundation for Research and Technology-Hellas (FORTH), GR70013 Heraklion, Crete, Greece.
*E-mail addresses:* filagg@iesl.forth.gr (A. Philippidis), anglos@uoc.gr, anglos@iesl.forth.gr (D. Anglos).

https://doi.org/10.1016/j.microc.2026.117446
Received 9 December 2025; Received in revised form 23 January 2026; Accepted 17 February 2026
Available online 22 February 2026

ancient communities [9]. In particular, ancient DNA comprises a unique archive, storing information that may not be present any more in modern samples. It can be found primarily in hard tissues, for example, bone or teeth, which have been known to favor endogenous DNA preservation. An extractive procedure is followed for obtaining DNA from the hard tissue, however, efficient extraction typically requires the partial or complete destruction of valuable and unique archaeological specimens. Therefore the success of large-scale genomic analyses of ancient human populations is partly based on advances in informed sample selection and proper bone sampling methods [1,10].

Several studies have shown that the cementum of the dental root preserves DNA better than other parts of the tooth [11–13]. Being the outer part of the root (Fig. 1B), the cementum is susceptible to degradation, especially when teeth have been found detached from the jaw, and in such cases it is often difficult to correctly assess the degree of preservation just by visual means. Certainly, the destructive character of ancient DNA analysis constitutes a significant concern, particularly so, when rare and precious samples are treated, and moreover when considering the frequently poor preservation of DNA [14,15]. As a result, the considerable operational costs for ancient DNA analysis combined with the often minimal or vanishing endogenous DNA yields can limit substantially the number of samples that can be analyzed in the context of an aDNA project. To circumvent these limitations, researchers have employed mass spectrometry (palaeoproteomics) [16–18] as well as spectrochemical methods such as Near-Infrared (NIR), Fourier-transform Infrared (FT-IR), Raman and Laser-induced breakdown spectroscopy (LIBS) [19–21] as alternatives for studying skeletal remains, in a minimally invasive manner, with remarkable results [22–24], but obviously not obtaining direct genetic information. Interestingly, Surface-enhanced Raman scattering has been applied in biomolecular and genetic studies, for example, SERS-enabled molecular identification based on DNA barcoding in *Hippocampus trimaculatus* samples [25].

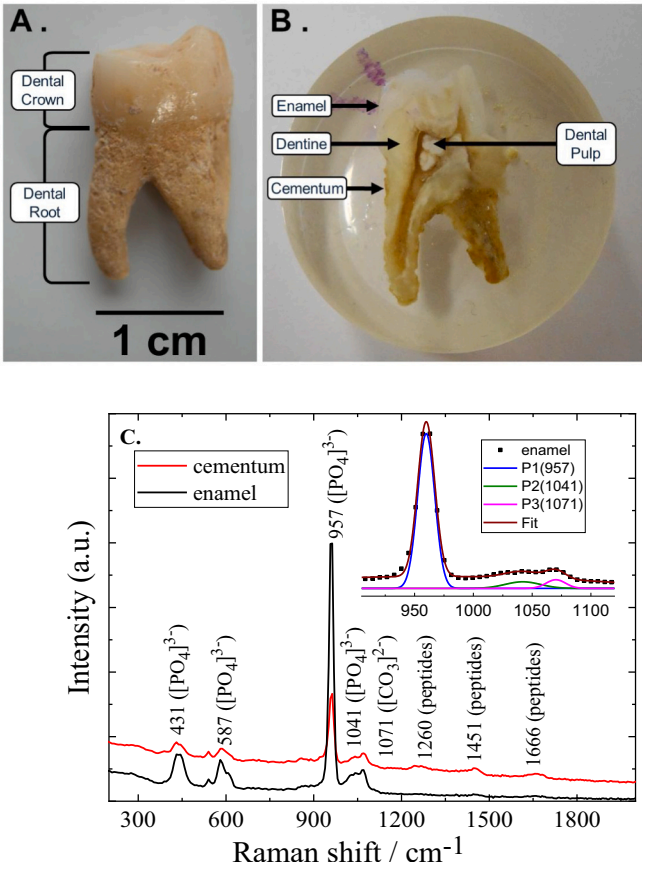


**Fig. 1.** Images of a tooth (molar) illustrating its different parts (A), a cross-section of the same tooth, embedded in resin, indicating the different tissues targeted for analyses (B) and typical Raman spectra collected from an ancient tooth (ADNA 100014_3) with characteristic vibrational bands indicated. Two different regions of the tooth have been analyzed: cementum (red line) and enamel (black line) (C). (For interpretation of the references to colour in this figure legend, the reader is referred to the web version of this article.)

In recent research work, Kontopoulos et al. [22] and Scaggion et al. [26] have suggested that FT-IR spectroscopy, based on the use of relevant spectral features and corresponding spectral indices, has the capacity to serve as a rapid screening tool for assessing the degree of collagen preservation in archaeological bone prior to performing C and N stable isotope ratio analyses and subsequently relating the levels of collagen with the preserved endogenous DNA. Indeed various studies have proposed specific FT-IR spectral indices relating to the presence of collagen in human and animal hard tissues, and indirectly to the preservation of endogenous DNA. For example, a) the infrared splitting factor [IRSF] and FW85% parameter, which evaluate relative changes in the structure of bioapatite [27], b) the carbonate-to-phosphate [C/P] ratio, a relative measure of carbonate content in bioapatite crystals [28], and c) the amide-to-phosphate ratio [Am/P], representative of the relative protein content of the apatite, have been utilized to estimate the degree of organic matter preservation in bone samples [29,30]. Similarly, Lescovar et al. [23] used ATR-FTIR, in combination with machine learning (ML) methods, as a pre-screening tool indicating DNA preservation in skeletal remains, including human bones and teeth. Furthermore, ML algorithms applied to FT-IR spectral data have proven to be effective in screening archaeological bones prior to ZooMS (Zooarchaeology by Mass Spectrometry) collagen analysis and aDNA analysis [24]. FT-IR spectroscopy has also been used to assess changes in the physicochemical properties of bones and teeth from various origins and time periods [31].

A recent review by Anzellini [32] examines how various spectroscopic techniques, such as FT-IR, Raman, or Fluorescence emission spectroscopy, LIBS, as well as X-ray diffractometry have been used by researchers in order to assess the levels of diagenesis in archaeological bones. Among these, FT-IR and Raman spectroscopy are found as the ones offering key advantages since they are easy-to-apply, most reliable, and least destructive. In a representative study, FT-Raman spectroscopy was employed in the analysis of ancient human teeth from archaeological sites dating from the 4th to 16th centuries CE, in order to investigate changes in the organic and inorganic composition of dental tissue over time. The results were compared against those collected from modern samples to assess the DNA preservation quality as a function of sample age [33]. On the basis of a specific band intensity ratio (average of amide I, $\delta(CH_2)$ and amide III to phosphate at 960 $cm^{-1}$) it was suggested that the conformation of the collagen component, in the ancient teeth, remained unchanged irrespective of burial age. In the context of a similar study, Raman spectroscopy was used to estimate the age of archaeological teeth (using the intensity ratio of the phosphate band at 963 $cm^{-1}$ to the organic CH band at 2950 $cm^{-1}$), and the results were compared with accelerator mass spectrometry (AMS) data, presenting high sensitivity to both the organic and mineral components of dental tissue [34]. A reliable protocol for accurately determining the sex of the deceased has been reported, combining proteomic analysis, archaeological evidence, and anthropological data from bone remains in several graves at a Greek cemetery at Reggio Calabria, Italy [35]. In the same study, an attempt was also undertaken to estimate the age of the deceased based on a detailed evaluation of Raman spectral data collected from bone samples. On the basis of the quantity of carbonate apatite, particularly the level of A-substituted apatite, a rough discrimination was possible concerning three individuals assessed as significantly younger compared to the rest and two more assessed as potentially the oldest ones. Very encouraging findings have been presented by Pestle et al. [36,37] as regards the use of a hand-held Raman spectrometer, which was employed as a pre-screening tool modeling the

levels of human bone collagen from archaeological samples on the basis of a simple linear function of the amide I, $\delta(CH_2)$, to the phosphate band ratio, showing high discrimination between well- and poorly preserved samples. Moreover, benchtop and handheld Raman spectrometers were used to examine the same set of 37 archaeological human bone samples in order to establish standardized data reporting protocols [38]. Likewise NIR spectroscopy, based on portable systems, has been applied to the quantification of collagen content and the chronological classification of ancient bone specimens (500 to 45,000 years old) [20,39]. NIR radiation provides the advantage of optical penetration depth (on the order of mm) [20] which secures more efficient probing of the dental tissue. Moreover, the combination of NIR spectroscopy with statistical methods such as Partial Least Squares Regression (PLSR) and Random Forest (RF) modeling, enables high-throughput bone screening and improves sample selection efficiency [39]. Similarly, exploring NIR hyperspectral imaging, coupled to normalized difference image (NDI) data processing, Sciutto and coworkers have been able to map collagen in archaeological bones [40]. Finally, Hoke et al. [41] have utilized the UV-induced autofluorescence of bones, to estimate their microstructure preservation, based on simple visual observation of the blue emission. This offered a screening method to identify samples containing well-preserved biomolecules.

In this paper, a new study is reported investigating the applicability and reliability of Raman spectroscopy as a rapid screening tool for indirectly estimating the amount of endogenous human DNA in ancient teeth by measuring their protein content relative to the inorganic matrix. This is the first time Raman spectroscopy is used in such a context, directly on the archaeological sample and with no pre-treatment other than cleaning for removing surface deposits. Spectra were obtained using excitation in the near infrared (NIR) range, at $\lambda = 1064$ nm, to minimize potential interference due to fluorescence emissions, either originating from environmental impurities or being intrinsic to the sample. Raman spectroscopy offers researchers the opportunity to conduct measurements in a short time (typical analysis time $< 5$ min), whereas with the development of reliable portable spectrometers, it provides the potential for performing field measurements. It is, furthermore, a non-destructive probe applied directly onto the sample surface (it just requires optical contact) with no need for any sample processing, such as extraction or fragmentation. Raman spectra exhibit well-resolved, distinct bands characteristic of both the inorganic (mainly of hydroxyapatite) and the proteinaceous (primarily comprising collagen residues) [42] components of the teeth. From the corresponding Raman bands, we have established relevant spectroscopic indices that are linked to the level of endogenous human DNA preservation and thus propose threshold values for these indicators, which suggest dental samples that are appropriate for archaeogenomic analysis, namely, samples with a higher likelihood of yielding substantial endogenous DNA. The results are highly promising, indicating that the proposed methodology can serve as a reliable tool for pre-screening dental samples in the context of ancient DNA analysis.

## 2. Materials and methods

### 2.1. Samples and general workflow

A total of 59 dental samples were used in this study ($n = 59$). These represented different types of teeth, molars, premolars, canines, and incisors, belonging to both male and female individuals. They originated from various archaeological excavation sites in Greece, dated to a wide time span, from 8800 BCE to 1941 CE. The actual DNA preservation level was determined via aDNA analyses in the Ancient DNA Lab (aDNA-lab) of IMBB-FORTH. The assessment of DNA preservation is based on the endogenous human DNA content, taking into account ancient DNA authentication indices (i.e., DNA sequence length distribution and *post-mortem* cytosine deamination rates) in order to confirm with certainty the ancient origin of the genetic material. For 49 of the samples (set A), endogenous human aDNA values were available prior to Raman analysis either from published studies or from unpublished data of the aDNA-lab (Table 1). These samples span a broad range of DNA preservation levels, from nearly zero up to 65%, and this minimizes biased sampling. In some specimens, the preserved enamel surface was extremely limited in size, preventing proper data acquisition from that part of the tooth. In all, enamel Raman spectra have been collected from 41 teeth while cementum spectra have been obtained from 45 teeth out of the 49 in set A (Table S1). In order to validate and assess the proposed approach, an additional set of 10 dental samples (Set B, Table 2) were treated as unknowns and were analyzed using Raman spectroscopy, prior to aDNA analysis. Their potential endogenous DNA content was estimated on the basis of spectroscopic indicators derived from the analysis of the aforementioned 49 samples. Additionally, four modern tooth samples from four different individuals were also analyzed to compare their spectroscopic index values against those derived from the archaeological samples. To eliminate potential interference from microbial and organic contaminants, modern teeth were sterilized by immersion in sodium hypochlorite solution for 24 h.

### 2.2. Ancient DNA analysis

Sampling permits for all archaeological samples (Tables 1 and 2) were granted by the Directorate of Conservation of Ancient and Modern Monuments (Ministry of Culture). All samples were processed according to established procedures and protocols [43–48]. In particular, while processing teeth for ancient DNA analysis, the non-destructive protocol of Harney et al. [49] was followed according to which a part of the dental root was protected with parafilm, and maintained for in situ Raman analysis.

The computational analyses for estimating the endogenous human DNA content, using the raw sequence reads, were performed as detailed in Psonis et al. [2]. All analyses were performed as implemented in the mapache v.0.3.0 pipeline [50]. Results, with respect to endogenous DNA content per sample [proportion of mapped reads, including duplicates, from total collapsed reads (paired-end reads; PE) or total retained reads after adapter removal (single-end reads; SE)], are provided in Tables 1 and 2. The histogram in Fig. S1a shows the distribution of endogenous human DNA values for the 49 samples listed in Table 1. In order to demonstrate that these samples are indeed representative of the overall distribution of DNA content (i.e. that most samples have low DNA values, below 10%), we constructed an additional histogram based on DNA content data from a larger set of 116 samples, which includes the 49 Raman-analyzed samples and additionally 67 samples (not Raman-analyzed) but with their DNA content known, on the basis of analyses performed at the aDNA-lab (Fig. S1b). The similar distribution patterns in the histograms (Fig. S1) indicate that the Raman-analyzed subset is indeed representative of the overall sample population in terms of DNA preservation.

### 2.3. Raman analysis

Raman spectra were obtained with a mobile Raman spectrometer (B&W Tek). The system consists of: a) the excitation source, a continuous-wave laser emitting at $\lambda = 1064$ nm, with maximum power $P_{L,max} = 450$ mW and linewidth, FWHM $= 0.3$ nm (BRM-1064-450), b) the Raman probe, with 0.22 NA objective lens (BAC 102–1064-HT) which yields a laser spot size of $d \approx 85$ μm at the sample surface, and c) the detector, an InGaAs array covering the spectral range 1047–1450 nm (BTC 284 N-1064) integrated into a diffraction grating spectrograph, providing spectral coverage from 100 $cm^{-1}$ up to 2500 $cm^{-1}$ with a spectral resolution of 12 $cm^{-1}$. The working values for laser power, exposure time, and number of scans were determined through a systematic optimization of the experimental parameters, aiming to achieve a high signal-to-noise ratio (S/N). In the current study, the laser power was set to $P_L = 80$ mW, measured at the sample surface. Each acquisition

**Table 1**
List of dental samples (Set A) with Lab code numbers and corresponding information: dating and geographic location of the site, type of tooth and endogenous human DNA content.

| No* | DNA lab code (ADNA 100###)** | Chronological period | Geographic location | Tooth type | Endogenous Human DNA (%) |
|---|---|---|---|---|---|
| 1 | 002_1 | 450–400 BCE | Amvrakia, Epirus | Premolar | 0.10 |
| 2 | 004 | 425–100 BCE | Amvrakia, Epirus | Canine | 0.09 |
| 3 | 010 | 425–400 BCE | Amvrakia, Epirus | Canine | 0.04 |
| 4 | 013_1 | 200–150 BCE | Amvrakia, Epirus | Premolar | 19.40 |
| 5 | 014_3 | 200–125 BCE | Amvrakia, Epirus | Incisor | 60.43 |
| 6 | 016_2 | 250–200 BCE | Amvrakia, Epirus | Canine | 2.01 |
| 7 | 030 | 1450–1300 BCE | Knossos, Crete | Tooth | 7.33 |
| 8 | 059 | 4100–3250 BCE | Tharrounia cave, Euboea Isl. | Premolar | 65.61 |
| 9 | 061 | 2700–2200 BCE | Perachora, Peloponnese | Molar | 4.75 |
| 10 | 064 | 2700–2200 BCE | Perachora, Peloponnese | Molar | 0.16 |
| 11 | 128_2 | 450–425 BCE | Amvrakia, Epirus | 3rd Molar | 20.73 |
| 12 | 135 | 475–450 BCE | Amvrakia, Epirus | Molar | 1.52 |
| 13 | 138 | 375–325 BCE | Amvrakia, Epirus | Molar | 0.49 |
| 14 | 142_4 | 8800–8600 BCE | Kouvaras cave, Attika, Central Greece | Premolar | 0.02 |
| 15 | 160 | 500–480 BCE | Tenea, Peloponnese | Molar | 24.61 |
| 16 | 161 | 27 BCE-476 CE | Tenea, Peloponnese | Molar | 8.49 |
| 17 | 162 | 150–100 BCE | Tenea, Peloponnese | Molar | 24.62 |
| 18 | 163 | 323–31 BCE | Tenea, Peloponnese | Incisor | 48.36 |
| 19 | 165 | 550–500 BCE | Tenea, Peloponnese | Molar | 6.44 |
| 20 | 177 | ~5500 BCE | Mesa Katsambas, Crete | Molar | 0.02 |
| 21 | 180 | ~5500 BCE | Mesa Katsambas, Crete | Canine | 0.03 |
| 22 | 181 | ~5500 BCE | Mesa Katsambas, Crete | Canine | 0.08 |
| 23 | 183 | ~5500 BCE | Mesa Katsambas, Crete | Incisor | 0.00 |
| 24 | 184 | ~5500 BCE | Mesa Katsambas, Crete | Premolar | 0.06 |
| 25 | 185 | ~5500 BCE | Mesa Katsambas, Crete | Premolar | 1.40 |
| 26 | 258_2 | 1941 CE | Sarakina (Adele), Crete | Molar | 6.24 |
| 27 | 261_2 | 1941 CE | Sarakina (Adele), Crete | Molar | 15.27 |
| 28 | 261_3 | 1941 CE | Sarakina (Adele), Crete | Molar | 7.23 |
| 29 | 263_2 | 1941 CE | Sarakina (Adele), Crete | Molar | 3.79 |
| 30 | 263_3 | 1941 CE | Sarakina (Adele), Crete | Molar | 9.31 |
| 31 | 267_1 | 1941 CE | Sarakina (Adele), Crete | Molar | 4.12 |
| 32 | 267_2 | 1941 CE | Sarakina (Adele), Crete | Premolar | 48.81 |
| 33 | 267_3 | 1941 CE | Sarakina (Adele), Crete | Premolar | 59.96 |
| 34 | 269_2 | 1941 CE | Sarakina (Adele), Crete | Molar | 24.71 |
| 35 | 270_2 | 1941 CE | Sarakina (Adele), Crete | Molar | 15.47 |
| 36 | 271_1 | 1941 CE | Sarakina (Adele), Crete | Molar | 16.87 |
| 37 | 273_1 | 1941 CE | Sarakina (Adele), Crete | Molar | 1.30 |
| 38 | 275_1 | 1941 CE | Sarakina (Adele), Crete | Canine | 6.08 |
| 39 | 276_1 | 1941 CE | Sarakina (Adele), Crete | Premolar | 38.24 |
| 40 | 276_2 | 1941 CE | Sarakina (Adele), Crete | Molar | 48.38 |
| 41 | 277_1 | 1941 CE | Sarakina (Adele), Crete | Incisor | 17.98 |
| 42 | 315_1 | 1941 CE | Sarakina (Adele), Crete | Incisor | 1.88 |
| 43 | 313_1 | 1941 CE | Sarakina (Adele), Crete | Canine | 20.48 |
| 44 | 314_2 | 1941 CE | Sarakina (Adele), Crete | Molar | 30.15 |
| 45 | 312_1 | 1941 CE | Sarakina (Adele), Crete | Molar | 12.76 |
| 46 | 314_1 | 1941 CE | Sarakina (Adele), Crete | Molar | 1.66 |
| 47 | 313_2 | 1941 CE | Sarakina (Adele), Crete | Molar | 15.43 |
| 48 | 312_2 | 1941 CE | Sarakina (Adele), Crete | Molar | 17.19 |
| 49 | 315_2 | 1941 CE | Sarakina (Adele), Crete | Molar | 39.88 |

* Samples 1–6, 11–13, and 15–19 are presented in a recent publication [Psonis et al., *BioRxiv* 2025] [9]. Samples 7 and 14 are part of an ongoing study currently in preparation for publication [Psonis et al.]. Samples 8–10 and 20–25 have been screened as part of pilot projects [aDNA-lab, IMBB-FORTH]. Samples 26–49 have already been presented in a previous publication [Psonis et al., *Forensic Science International: Genetics* 2024] [2].

** Sample codes have been abbreviated for the sake of simplicity as ADNA 100###, where ### corresponds to the final part of the original sample code.

had a typical exposure time of $\tau = 30$ s, and 2 scans were performed at each analyzed position. Although teeth consist of three tissue types (enamel, cementum and dentine, the latter located internally, Fig. 1B), this study presents results only from measurements obtained on the cementum (external surface of dental root) and enamel (external surface of dental crown). For each region analyzed, three replicate measurements were acquired at different positions and the spectrum reported represents their average.

## 3. Results and discussion

Representative Raman spectra (100–1900 $cm^{-1}$) from the cementum and enamel regions of an archaeological dental sample (ADNA 100014_3) analyzed in this study are shown in Fig. 1C. Characteristic spectral bands corresponding to both the inorganic matrix and the organic component of the tooth are evident. The inorganic part, mainly hydroxyapatite [$Ca_5(PO_4)_3(OH)$], exhibits bands at relatively low frequencies (wavenumbers), more specifically at 431, 587, 957, and 1041 $cm^{-1}$. These are all due to vibrations of the phosphate group $[PO_4]^{3-}$ and assigned to symmetric bending ($\nu_2$), antisymmetric bending ($\nu_4$), symmetric stretching ($\nu_1$), and antisymmetric stretching ($\nu_3$), respectively [33]. The Raman band at 1071 $cm^{-1}$ corresponds to vibration of the tooth carbonate component $[CO_3]^{2-}$ and particularly to the symmetric stretching ($\nu_1$). The organic component primarily consists of proteins, typically collagen residues, and exhibits bands in the spectral range 1200–1700 $cm^{-1}$ all due to peptide bond vibrations. In particular, the band at 1260 $cm^{-1}$ is due to the C—N stretching and the N—H bending of the peptide bond, termed as amide III. The one at 1451 $cm^{-1}$ corresponds to the C—H scissoring vibration of glycine, while the one at 1666 $cm^{-1}$ corresponds to the C═O stretching (amide I) [33,51,52]. The experimental Raman data for all dental samples analyzed in this study are provided in the supplementary information.

**Table 2**
List of dental samples (Set B), treated as unknowns, with Lab code numbers indicated and corresponding information: dating and geographic location of the site, type of tooth and endogenous human DNA content.

| No* | DNA lab code (ADNA 100###)** | Chronological period | Geographic location | Tooth type | Endogenous Human DNA (%) |
|---|---|---|---|---|---|
| 1 | 112_3 | 1500–1800 CE | Poros (Heraklion), Crete | Incisor | 0.06 |
| 2 | 113_5 | 1500–1800 CE | Poros (Heraklion), Crete | Premolar | 0.22 |
| 3 | 114_3 | 1500–1800 CE | Poros (Heraklion), Crete | Molar | 16.9 |
| 4 | 115_4 | 1500–1800 CE | Poros (Heraklion), Crete | Premolar | 0.43 |
| 5 | 115_5 | 1500–1800 CE | Poros (Heraklion), Crete | Premolar | 9.48 |
| 6 | 116_2 | 1500–1800 CE | Poros (Heraklion), Crete | Canine | 2.41 |
| 7 | 117_2 | 1500–1800 CE | Poros (Heraklion), Crete | Molar | 2.03 |
| 8 | 119_2 | 1500–1800 CE | Poros (Heraklion), Crete | Premolar | 3.24 |
| 9 | 120_3 | 1500–1800 CE | Poros (Heraklion), Crete | Molar | 0.74 |
| 10 | 122_3 | 1500–1800 CE | Poros (Heraklion), Crete | Premolar | 0.04 |

* Samples in Set B are part of an ongoing study currently in preparation for publication [aDNA-lab, IMBB-FORTH]. These 10 samples were treated as unknowns in the present study and were first analyzed using Raman spectroscopy. Subsequently, their endogenous human aDNA values were quantified.
** Sample codes have been abbreviated for the sake of simplicity as ADNA 100###, where ### corresponds to the final part of the original sample code.

Comparison of the Raman spectra from the cementum and enamel regions reveals profound differences in the 1200–1700 $cm^{-1}$ region. The three Raman bands, characteristic of the proteinaceous component of the tooth, are prevalent in the cementum rather than in the enamel, which contains hardly any organic matter. It is known [53,54] that cementum consists of 40% organic compounds, of which approximately 90% correspond to collagen. These collagen residues are responsible for the bands recorded in the Raman spectra of the cementum.

In the context of the present study, two Raman-derived indices are evaluated, reflecting the amide-to-phosphate [Am/P] and the carbonate-to-phosphate [C/P] ratios, both previously shown to have the potential to discriminate between bone samples, rich and poor in endogenous DNA, as overviewed in the Introduction [22].

As pointed out, spectra collected on the surface of the cementum, the protein-rich part of the tooth, show bands arising from the peptide bond vibrations. Therefore it is reasonable to select a spectral index reflecting the protein content preserved in the tooth relative to the inorganic matrix, such as the amide-to-phosphate [AmI/P] ratio, already used in relevant studies based on FT-IR and Raman analysis of archaeological bones. In our case, [AmI/P] corresponds to the intensity ratio of the amide I band at 1666 $cm^{-1}$ versus the phosphate band at 957 $cm^{-1}$, defined as:

$$[AmI/P] = I_{1666cm^{-1}}/I_{957cm^{-1}} \quad (1)$$

Fig. 2 presents graphs displaying values of [AmI/P] for the cementum and enamel regions of the teeth in Set A against values of the % aDNA. A comparison of the two graphs shows that [AmI/P] is consistently higher in the cementum than in the enamel, with mean values of 0.171 ± 0.065 and 0.049 ± 0.027, respectively. This observation is consistent with the low organic content of the enamel tissue. Pearson's and Spearman's correlation coefficients were calculated to assess the relationship between the spectral index values and the % endogenous DNA content. While no correlation was observed for the enamel region (Fig. 2b), the [AmI/P] values in cementum exhibited a weak but discernible correlation with DNA content (Fig. 2a), suggesting that this index may provide a useful criterion for prescreening samples prior to more extensive DNA analyses.

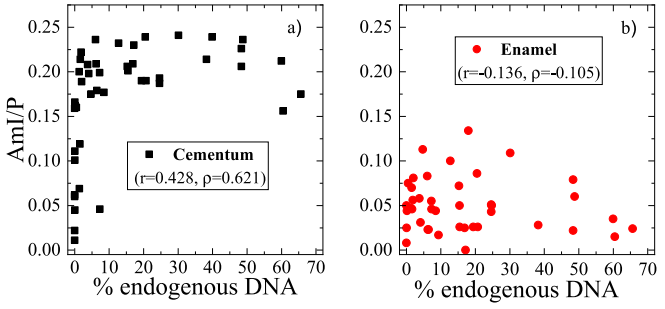


**Fig. 2.** Graphs showing values of the spectral index [AmI/P], for cementum (a) and enamel (b), obtained through Raman spectroscopy measurements, versus the percentage of endogenous human DNA. Pearson (r) and Spearman (ρ) correlation coefficients are given in the graphs.

The Γ-shaped correlation diagram for the cementum data (Fig. 2a) resembles the pattern observed by Kontopoulos et al. [22] in their study of archaeological bones via FT-IR spectroscopy, in which the infrared splitting factor (IRSF) is correlated with the endogenous DNA levels. In the context of the present study, we adopted a 5% DNA content threshold value, as indicative of good preservation of endogenous DNA. To establish the most effective index threshold, different values of [AmI/P] around its mean value were systematically evaluated, and their performance was assessed comparing predicted and actual DNA preservation classification (Fig. S2). The optimal threshold ratio value was determined to be $[AmI/P]_{th} = 0.17$, as it provided the most effective classification between poorly- and well-preserved human DNA of ancient dental samples, yielding an overall success of prediction of 80% (see also Fig. 2a). Specifically, using this $[AmI/P]_{th}$ value, 23 out of the 25 well-preserved teeth (92%) were correctly identified, and 13 out of the 20 poorly-preserved ones (65%) were correctly rejected. Table 3 presents the corresponding confusion matrix summarizing the classification results described above.

In comparison, Kontopoulos et al. [22] in their study, achieved a 93% success rate in identifying archaeological bones with endogenous DNA levels greater than 1%, on the basis of the carbonate-to-phosphate ratio, [C/P], extracted from FT-IR spectra. It is noted, however, that in that particular work bone samples were grinded into powder prior to analysis, whereas in the context of the approach proposed herein analysis is performed in situ, on the teeth themselves, non-invasively.

To further examine the strength of the current approach an alternative amide-to-phosphate ratio was also evaluated, using the amide III band at 1260 $cm^{-1}$, which is defined as:

$$[AmIII/P] = I_{1260cm^{-1}}/I_{957cm^{-1}} \quad (2)$$

As expected, this ratio yields comparable results, after optimization of the threshold value. With $[AmIII/P]_{th} = 0.086$ (and keeping the DNA

**Table 3**
Confusion matrix based on the graph in Fig. 2a (for $[AmI/P]_{th} = 0.17$ and a value of 5% to indicate the good endogenous human DNA preservation) illustrating the classification performance of the model.

| | Predicted as well-preserved | Predicted as poorly-preserved |
|---|---|---|
| Actual well-preserved (25) | **23** (True Positives) | 2 (False Negatives) |
| Actual poorly-preserved (20) | 7 (False Positives) | **13** (True Negatives) |

content threshold at 5%), 23 out of the 25 well-preserved teeth (92%) were correctly classified, while 9 of the 20 poorly-preserved teeth (45%) were correctly rejected (Fig. S3). These findings indicate that the use of either one of the two indices, [AmI/P] or [AmIII/P] provides reliable discrimination of samples according to their DNA preservation.

The choice of 5% DNA content threshold as a criterion for acceptance of samples as "DNA-rich" has been based on specific analytical requirements of the aDNA-lab. This value, however, can have an influence on the classification outcome. To further assess the robustness of the proposed Raman-based screening approach, alternative DNA content criteria were evaluated, setting the threshold at 1% and 10%. Following the methodology described above, an optimum $[AmI/P]_{th}$ value was calculated for each one of the DNA level criteria and a graphical summary of the classification results is displayed in Fig. 3 for DNA cutoff values at 1%, 5% and 10%.

As shown, the best overall accuracy, defined as the sum of true assignments (TP + TN), is obtained for the 1% DNA content threshold (91%), with all poorly preserved samples correctly rejected and 88% of the well-preserved teeth correctly classified. At the higher threshold of 5%, the overall accuracy decreases slightly to 80%, primarily due to a reduction in the correct classification of poorly preserved samples (65%), while well-preserved teeth are still accurately identified (92%). When the DNA content criterion is increased to 10%, the overall accuracy decreases further, to 76%, with 65% of the poorly preserved and 90% of the well-preserved teeth correctly classified. These results demonstrate that, although the exact DNA content criterion affects the quantitative performance metrics, the [AmI/P] index consistently provides reliable discrimination between well- and poorly-preserved teeth across this range of DNA cutoff values.

To further test the proposed methodology and more specifically in order to validate the [AmI/P] index as a reliable DNA screening tool, two additional experiments were conducted.

In the first test, Raman spectra of four modern teeth were obtained and the corresponding [AmI/P] index for cementum was found to have a mean value of 0.195 ± 0.048. As expected, given the young age of the samples, this value is above the estimated $[AmI/P]_{th}$ value of 0.17 corresponding to the 5% DNA criterion.

In the second test, Raman analysis of 10 archaeological teeth with unknown endogenous DNA content was carried out. The calculated [AmI/P] values for each sample are displayed in Fig. 4. The % of endogenous DNA of each sample, measured a posteriori, is also included in the graph.

Among the 10 archaeological teeth analyzed, all those with endogenous DNA content above 5% were correctly identified as well-preserved (TP). Three samples were misclassified as well-preserved despite containing less than 5% DNA (FP), while 5 poorly preserved teeth were correctly rejected (TN). The classification results are summarized in the confusion matrix presented in Table 4. This result highlights the high sensitivity of the Raman-based approach and the validity of the [AmI/P] index, ensuring that samples with sufficient DNA preservation are not inadvertently discarded during preliminary screening. Although some false positives were observed, this trade-off is acceptable for a prescreening tool, whereby avoiding the loss of valuable material is of primary importance.

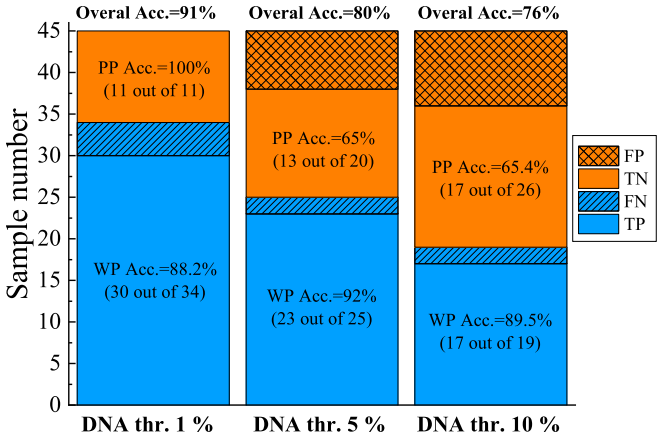


**Fig. 3.** Classification performance of the [AmI/P] index for different DNA content criteria (1%, 5%, and 10%). Bars show the number of correctly and incorrectly classified samples as true positives (TP), true negatives (TN), false positives (FP), and false negatives (FN). Graph includes the Well-Preserved (WP), Poorly-Preserved (PP) and overall accuracy percent for each case.

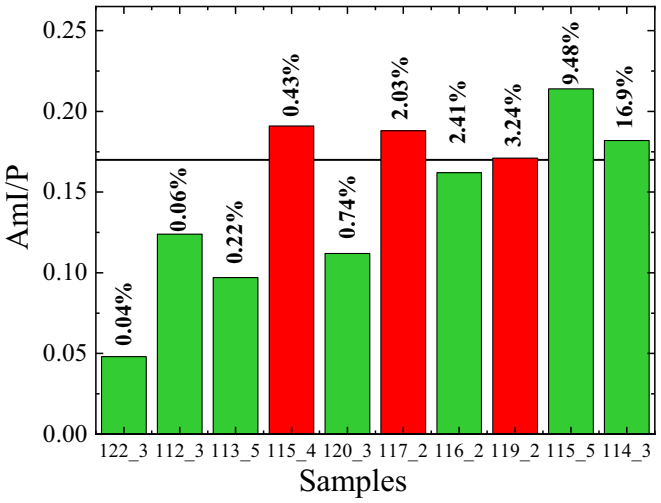


**Fig. 4.** Bar graph displaying [AmI/P] values for cementum for the teeth in Set B (see Table 2). The horizontal black line indicates the proposed value for $[AmI/P]_{th}$ which equals 0.17. The percentage of endogenous human DNA for all samples is also marked on each one of the bars. Green and red bars represent correctly classified tooth samples and misclassified ones respectively. (For interpretation of the references to colour in this figure legend, the reader is referred to the web version of this article.)

Next we checked the capacity of the [AmI/P] index to suggest sorting of teeth based on their age. All the samples listed in Table 1 were classified into three groups based on their chronological period. Specifically, the first group includes samples dated between 8800 and 1000 BCE, the second group consists of samples dated between 550 and 31 BCE, and the third group comprises modern samples dated to 1941 CE. The mean values of [AmI/P] (from the cementum) are 0.087 ± 0.061, 0.162 ± 0.037 and 0.214 ± 0.015 for the oldest, intermediate, and modern samples, respectively. The results are highly promising, as the [AmI/P] index exhibits a clear increasing trend from the oldest to the more recent samples, consistent with the expectation that the modern specimens retain a higher organic content.

The second index assessed in the context of this work was the [C/P] corresponding to the intensity ratio of the carbonate band at 1071 $cm^{-1}$ versus the phosphate band at 957 $cm^{-1}$, defined as:

$$[C/P] = I_{1071cm^{-1}}/I_{957cm^{-1}} \quad (3)$$

This index is indicative of the relative carbonate content in the teeth [28,30]. Since DNA molecules are known to be protected from degradation by adsorbing onto hydroxyapatite crystals, any structural or

**Table 4**
Confusion matrix for the endogenous DNA content prediction accuracy achieved through Raman analysis of the teeth in Set B, based on the bar graph in Fig. 4.

| | Predicted as well-preserved | Predicted as poorly-preserved |
|---|---|---|
| Actual well-preserved (2) | **2** (True Positives) | 0 (False Negatives) |
| Actual poorly-preserved (8) | 3 (False Positives) | **5** (True Negatives) |

compositional changes detected in these crystals reflected by [C/P] ratio, could potentially be associated with the preservation of endogenous DNA [22]. Fig. 5 displays values of [C/P] for cementum and enamel regions of the teeth of Set A against values of the % aDNA. The value of [C/P] is found to be higher in the cementum compared to the enamel region, with mean values of 0.281 ± 0.045 and 0.207 ± 0.027, respectively. Pearson's and Spearman's correlation coefficients were calculated to assess the relationship between the spectral index values and the % endogenous DNA content, but no correlations were observed in either region. Consequently, this spectral index does not provide a reliable basis for screening samples according to their endogenous DNA content under the present experimental conditions. However, it is important to note that the medium spectral resolution of the portable spectrometer, employed in the present study, may have affected the results. Specifically, the Raman band at 1041 $cm^{-1}$, corresponding to the phosphate anion vibrations, overlaps with the selected carbonate band at 1071 $cm^{-1}$ (see Fig. 1C), potentially introducing interference. Improved spectral resolution, typically available with laboratory FT-Raman instruments, could mitigate this overlap and enhance the reliability of the results. An alternative approach, aiming to clean up the overlapping phosphate and carbonate bands features, by use of peak deconvolution algorithms, was explored (see Fig. 1C inset). However, under the current spectral resolution, even though deconvolution resulted in band separation the corrected values of the [C/P] index did not give rise to any correlation with the endogenous DNA content of the dental samples.

On the basis of the data presented Raman analysis is shown to be a valuable approach for the analysis of archaeological remains, complementary to other state-of-the-art methods, including mass spectrometry, FT-IR, or NIR spectroscopy techniques. A key point of the current approach is the choice of an excitation source in the NIR, 1064 nm. Despite the reduced Raman scattering efficiency, in comparison with excitation in the green or red, NIR excitation provides a distinct advantage related to minimization of fluorescence emission and furthermore results in more efficient penetration into the tissue. This is in agreement with observations by Pestle and coworkers, who have found excitation at 1030 nm or 1064 nm as more appropriate for performing Raman analysis of the proteinaceous component of archaeological bones [36,37].

## 4. Conclusion

The study presented herein demonstrates that Raman spectroscopy can serve as an effective pre-screening method for assessing endogenous DNA preservation in archaeological dental remains. Raman analysis can contribute to the development of a non-invasive approach, enabling field scientists to only select samples having high probability for human DNA preservation while, in parallel, avoiding unnecessary sample destruction. For the set of samples, examined in this study, the results obtained on the basis of the [AmI/P] index were highly encouraging. Setting a threshold for endogenous human DNA at 5%, which separated the DNA-rich versus the DNA-poor teeth, out of 25 samples with high aDNA preservation, the model correctly identified 23 (true positives), while only 2 were misclassified (false negatives). This corresponds to an accuracy of 92%, indicating that our approach is highly effective in detecting well-preserved samples. This approach demonstrated strong performance in the classification of unknown samples, achieving high accuracy with no false negatives. Effective pre-screening of samples will ensure that ancient DNA analysis is carried out exclusively on those dental remains that are most likely to yield significant amounts of endogenous DNA, thereby saving on person-hours and wet-lab expenses.

The next objective is to expand this study by analyzing additional samples from a wider range of geographical regions, burial environments and chronological periods. Increased variation in DNA preservation across the extended samples list is anticipated, reflecting differences in soil chemistry (e.g. pH), moisture levels, climatic conditions and other taphonomic factors. Future work of this kind will be crucial for further assessing the influence of diagenesis and for validating the applicability of the proposed method. Additionally, it is possible to explore alternative spectral indices and also employ a spectrometer with a broader spectral range extending out to 3200 $cm^{-1}$ to include the CH streching vibration bands. Combination of Raman with NIR analysis data is worthy of a thorough investigation considering the potential of complementarity in providing more reliable predictions concerning the presence of endogenous genetic material in teeth. Finally, a more global treatment of spectral data based on machine learning algorithms is under investigation in an effort to increase further the potential of accurate sample pre-screening.

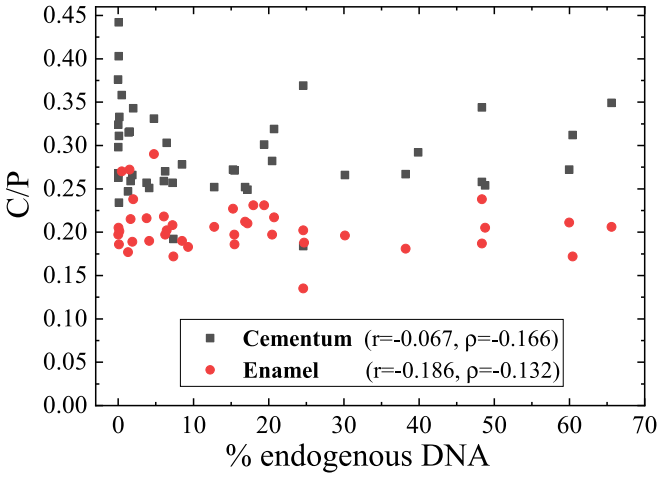


**Fig. 5.** Graph showing values of the [C/P] spectral index (calculated based on the Raman data from Set A), versus the corresponding percentage of endogenous human DNA for both cementum and enamel. Pearson (r) and Spearman (ρ) correlation coefficients are provided.

## CRediT authorship contribution statement

**Aggelos Philippidis:** Writing – review & editing, Writing – original draft, Visualization, Validation, Methodology, Investigation, Formal analysis. **Angeliki Mamali:** Investigation, Formal analysis. **Victor Pinon:** Writing – review & editing, Visualization, Validation, Methodology, Formal analysis. **Despoina Vassou:** Writing – review & editing, Validation, Resources, Methodology, Investigation. **Argyro Nafplioti:** Writing – review & editing. **Eugenia Tabakaki:** Writing – review & editing. **Nikos Poulakakis:** Writing – review & editing, Project administration, Funding acquisition, Conceptualization. **Alexandros Stamatakis:** Writing – review & editing, Resources, Funding acquisition. **Pavlos Pavlidis:** Writing – review & editing. **Nikolaos Psonis:** Writing – review & editing, Methodology, Formal analysis, Data curation. **Demetrios Anglos:** Writing – review & editing, Supervision, Project administration, Funding acquisition, Conceptualization.

## Ethics declaration

The research team conducted work involving human remains in full compliance with the ethical standards outlined in the European Code of Conduct for Research Integrity (2023), as well as the globally applicable ethical guidelines proposed by Alpaslan-Roodenberg et al. [55] Ethical approval for the study was obtained from the Research Ethics Committee of the Foundation for Research and Technology – Hellas (FORTH), under protocol number REC 149/29-06-2022.

## Funding

Theodore Papazoglou FORTH Synergy Grants, Call 2022,

Spectroscopic Screening of Ancient Dental Remains for Optimized Archaeogenetic Analysis, “Spectra-Gen”.

“ReMade@ARI”, Funded by the European Union as part of the Horizon Europe call HORIZON-INFRA-2021-SERV-01 under grant agreement number 101058414 and co-funded by UK Research and Innovation (UKRI) under the UK government's Horizon Europe funding guarantee (grant number 10039728) and by the Swiss State Secretariat for Education, Research and Innovation (SERI) under contract number 22.00187. Views and opinions expressed are however those of the author(s) only and do not necessarily reflect those of the European Union or the UK Science and Technology Facilities Council or the Swiss State Secretariat for Education, Research and Innovation (SERI). Neither the European Union nor the granting authorities can be held responsible for them.

HELLAS-CH project (MIS 5002735), implemented under the “Action for Strengthening Research and Innovation Infrastructures,” funded in the context of the National Strategic Reference Framework, Operational Programme “Competitiveness, Entrepreneurship and Innovation” (NSRF 2014–2020), and co-financed by Greece and the EU (European Regional Development Fund).

SpArch project (Spectrochemical Analysis of Archaeological Bio-Organic Residues, HFRI-FM17-TΔE-3542) financed by the Hellenic Foundation for Research and Innovation (HFRI) under the “1st Call for HFRI Research Projects to support Faculty members and Researchers”.

European Union (EU) ERA chair program, under Grant Agreement No. 101087081 (Comp-Biodiv-GR).

## Declaration of competing interest

The authors declare that they have no known competing financial interests or personal relationships that could have appeared to influence the work reported in this paper.

## Acknowledgments

This research was made possible through the generous contribution of the Ephorates of Antiquities of Heraklion, Corinth, and Arta, the Ephorate of Palaeoanthropology and Speleology - Greece, as well as the Adele Community (Rethymno, Crete) who gave permissions and provided the bioarchaeological material essential for our study.

The authors would like to thank L. Spanos for providing the modern tooth samples analyzed in this study. The authors are indebted to Dr. M. Velegrakis (IESL-FORTH) for permitting access to the mobile Raman instrument used in this study.

## Appendix A. Supplementary data

Supplementary data to this article can be found online at https://doi.org/10.1016/j.microc.2026.117446.

## Data availability

Research Link Provided
raw Raman data (Original data) (zenodo)

## References

[1] L. Orlando, R. Allaby, P. Skoglund, C. Der Sarkissian, P.W. Stockhammer, M. C. Ávila-Arcos, Q. Fu, J. Krause, E. Willerslev, A.C. Stone, C. Warinner, Ancient DNA analysis, Nat. Rev. Methods Primers 1 (2021) 14, https://doi.org/10.1038/s43586-020-00011-0.

[2] N. Psonis, D. Vassou, A. Nafplioti, E. Tabakaki, P. Pavlidis, A. Stamatakis, N. Poulakakis, Identification of the 18 world war II executed citizens of Adele, Rethymnon, Crete using an ancient DNA approach and low coverage genomes, Forensic Sci. Int. Genet. 71 (2024) 103060, https://doi.org/10.1016/j.fsigen.2024.103060.

[3] D. Koptekin, E. Yüncü, R. Rodríguez-Varela, N.E. Altınışık, N. Psonis, N. Kashuba, S. Yorulmaz, R. George, D.D. Kazancı, D. Kaptan, K. Gürün, K.B. Vural, H. C. Gemici, D. Vassou, E. Daskalaki, C. Karamurat, V.K. Lagerholm, Ö.D. Erdal, E. Kırdök, A. Marangoni, A. Schachner, H. Üstündağ, R. Shengelia, L. Bitadze, M. Elashvili, E. Stravopodi, M. Özbaşaran, G. Duru, A. Nafplioti, C.B. Rose, T. Gencer, G. Darbyshire, A. Gavashelishvili, K. Pitskhelauri, Ö. Çevik, O. Vuruşkan, N. Kyparissi-Apostolika, A.M. Büyükkarakaya, U. Oğuzhanoğlu, S. Günel, E. Tabakaki, A. Aliev, A. Ibrahimov, V. Shadlinski, A. Sampson, G. M. Kılınç, Ç. Atakuman, A. Stamatakis, N. Poulakakis, Y.S. Erdal, P. Pavlidis, J. Storå, F. Özer, A. Götherström, M. Somel, Spatial and temporal heterogeneity in human mobility patterns in Holocene Southwest Asia and the East Mediterranean, Curr. Biol. 33 (2023) 41–57, https://doi.org/10.1016/j.cub.2022.11.034.

[4] N. Psonis, D. Vassou, L. Nicolaou, S. Roussiakis, G. Iliopoulos, N. Poulakakis, S. Sfenthourakis, Mitochondrial sequences of the extinct Cypriot pygmy hippopotamus confirm its phylogenetic placement, Zool. J. Linnean Soc. 196 (2022) 979–989, https://doi.org/10.1093/zoolinnean/zlab089.

[5] F. Clemente, M. Unterländer, O. Dolgova, C.E.G. Amorim, F. Coroado-Santos, S. Neuenschwander, E. Ganiatsou, D.I. Cruz Dávalos, L. Anchieri, F. Michaud, L. Winkelbach, J. Blöcher, Y.O. Arizmendi Cárdenas, B. Sousa Da Mota, E. Kalliga, A. Souleles, I. Kontopoulos, G. Karamitrou-Mentessidi, O. Philaniotou, A. Sampson, D. Theodorou, M. Tsipopoulou, I. Akamatis, P. Halstead, K. Kotsakis, D. Urem-Kotsou, D. Panagiotopoulos, C. Ziota, S. Triantaphyllou, O. Delaneau, J.D. Jensen, J.V. Moreno-Mayar, J. Burger, V.C. Sousa, O. Lao, A.-S. Malaspinas, C. Papageorgopoulou, The genomic history of the Aegean palatial civilizations, Cell 184 (2021) 2565–2586, https://doi.org/10.1016/j.cell.2021.03.039.

[6] V. Staikou, P.D. Sianis, D. Vassou, N. Psonis, M.E. Allentoft, G. Iliopoulos, Middle Helladic tombs at Nydri plain, Lefkas Island, An Archaeological and Paleoanthropological Study, JGA 6 (2021) 43–60, https://doi.org/10.32028/9781789698886-4.

[7] C. Hedenstierna-Jonson, A. Kjellström, T. Zachrisson, M. Krzewińska, V. Sobrado, N. Price, T. Günther, M. Jakobsson, A. Götherström, J. Storå, A female Viking warrior confirmed by genomics, American. J Phys. Anthropol. 164 (2017) 853–860, https://doi.org/10.1002/ajpa.23308.

[8] K.-G. Sjögren, I. Olalde, S. Carver, M.E. Allentoft, T. Knowles, G. Kroonen, A.W. G. Pike, P. Schröter, K.A. Brown, K.R. Brown, R.J. Harrison, F. Bertemes, D. Reich, K. Kristiansen, V. Heyd, Kinship and social organization in copper age Europe. A cross-disciplinary analysis of archaeology, DNA, isotopes, and anthropology from two Bell Beaker cemeteries, PLoS One 15 (2020) e0241278, https://doi.org/10.1371/journal.pone.0241278.

[9] N. Psonis, E. Tabakaki, D. Vassou, S. Papadantonakis, A. Souleles, A. Nafplioti, G. Kousis Tsampazis, A. Papadopoulou, K. Xanthopoulos, P. Panailidis, A. Georgiadou, D. Papakosta, S. Koursioti, M. Evangelinou, V. Papadopoulou, P. Evaggeloglou, E. Korka, I. Christidis, M. Ioannou, T. Kontogianni, A. Arkoumanis, A. Stamatakis, N. Poulakakis, C. Papageorgopoulou, P. Pavlidis, Genetic affinities between the ancient Greek colony of Amvrakia and its metropolis, Genome Biol. (2026), https://doi.org/10.1186/s13059-026-03968-5.

[10] H.B. Hansen, P.B. Damgaard, A. Margaryan, J. Stenderup, N. Lynnerup, E. Willerslev, M.E. Allentoft, Comparing ancient DNA preservation in petrous bone and tooth cementum, PLoS One 12 (2017) e0170940, https://doi.org/10.1371/journal.pone.0170940.

[11] C.J. Adler, W. Haak, D. Donlon, A. Cooper, Survival and recovery of DNA from ancient teeth and bones, J. Archaeol. Sci. 38 (2011) 956–964, https://doi.org/10.1016/j.jas.2010.11.010.

[12] D. Higgins, J.J. Austin, Teeth as a source of DNA for forensic identification of human remains: a review, Sci. Justice 53 (2013) 433–441, https://doi.org/10.1016/j.scijus.2013.06.001.

[13] D. Higgins, J. Kaidonis, G. Townsend, T. Hughes, J.J. Austin, Targeted sampling of cementum for recovery of nuclear DNA from human teeth and the impact of common decontamination measures, Investig. Genet. 4 (2013) 18, https://doi.org/10.1186/2041-2223-4-18.

[14] A.W. Briggs, U. Stenzel, P.L.F. Johnson, R.E. Green, J. Kelso, K. Prüfer, M. Meyer, J. Krause, M.T. Ronan, M. Lachmann, S. Pääbo, Patterns of damage in genomic DNA sequences from a Neandertal, Proc. Natl. Acad. Sci. USA 104 (2007) 14616–14621, https://doi.org/10.1073/pnas.0704665104.

[15] J. Dabney, M. Meyer, S. Paabo, Ancient DNA damage, Cold Spring Harb. Perspect. Biol. 5 (2013) a012567, https://doi.org/10.1101/cshperspect.a012567.

[16] J. Hendy, Ancient protein analysis in archaeology, Sci. Adv. 7 (2021) eabb9314, https://doi.org/10.1126/sciadv.abb9314.

[17] J. Hendy, F. Welker, B. Demarchi, C. Speller, C. Warinner, M.J. Collins, A guide to ancient protein studies, Nat Ecol Evol 2 (2018) 791–799, https://doi.org/10.1038/s41559-018-0510-x.

[18] K. McGrath, K. Rowsell, C. Gates St-Pierre, A. Tedder, G. Foody, C. Roberts, C. Speller, M. Collins, Identifying archaeological bone via non-destructive ZooMS and the materiality of symbolic expression: examples from Iroquoian bone points, Sci. Rep. 9 (2019) 11027, https://doi.org/10.1038/s41598-019-47299-x.

[19] G. Festa, C. Andreani, M. Baldoni, V. Cipollari, C. Martínez-Labarga, F. Martini, O. Rickards, M.F. Rolfo, L. Sarti, N. Volante, R. Senesi, F.R. Stasolla, S.F. Parker, A. R. Vassalo, A.P. Mamede, L.A.E. Batista De Carvalho, M.P.M. Marques, First analysis of ancient burned human skeletal remains probed by neutron and optical vibrational spectroscopy, Sci. Adv. 5 (2019) eaaw1292, https://doi.org/10.1126/sciadv.aaw1292.

[20] M. Sponheimer, C.M. Ryder, H. Fewlass, E.K. Smith, W.J. Pestle, S. Talamo, Saving old bones: a non-destructive method for bone collagen prescreening, Sci. Rep. 9 (2019) 13928, https://doi.org/10.1038/s41598-019-50443-2.

[21] P. Siozos, N. Hausmann, M. Holst, D. Anglos, Application of laser-induced breakdown spectroscopy and neural networks on archaeological human bones for

the discrimination of distinct individuals, J. Archaeol. Sci. Rep. 35 (2021) 102769, https://doi.org/10.1016/j.jasrep.2020.102769.
[22] I. Kontopoulos, K. Penkman, V.E. Mullin, L. Winkelbach, M. Unterländer, A. Scheu, S. Kreutzer, H.B. Hansen, A. Margaryan, M.D. Teasdale, B. Gehlen, M. Street, N. Lynnerup, I. Liritzis, A. Sampson, C. Papageorgopoulou, M.E. Allentoft, J. Burger, D.G. Bradley, M.J. Collins, Screening archaeological bone for palaeogenetic and palaeoproteomic studies, PLoS One 15 (2020) e0235146, https://doi.org/10.1371/journal.pone.0235146.
[23] T. Leskovar, I. Zupanič Pajnič, Ž.M. Geršak, I. Jerman, M. Črešnar, ATR-FTIR spectroscopy combined with data manipulation as a pre-screening method to assess DNA preservation in skeletal remains, Forensic Sci. Int. Genet. 44 (2020) 102196, https://doi.org/10.1016/j.fsigen.2019.102196.
[24] M. Pal Chowdhury, K.D. Choudhury, G.P. Bouchard, J. Riel-Salvatore, F. Negrino, S. Benazzi, L. Slimak, B. Frasier, V. Szabo, R. Harrison, G. Hambrecht, A. C. Kitchener, R.A. Wogelius, M. Buckley, Machine learning ATR-FTIR spectroscopy data for the screening of collagen for ZooMS analysis and mtDNA in archaeological bone, J. Archaeol. Sci. 126 (2021) 105311, https://doi.org/10.1016/j.jas.2020.105311.
[25] Q. Wang, Y. Wu, Y. Wang, R. Mei, R. Zhao, X. Wang, L. Chen, Surface enhanced Raman scattering tag enabled ultrasensitive molecular identification of Hippocampus trimaculatus based on DNA barcoding, Talanta 294 (2025) 128289, https://doi.org/10.1016/j.talanta.2025.128289.
[26] C. Scaggion, M. Marinato, G. Dal Sasso, L. Nodari, T. Saupe, S. Aneli, L. Pagani, C. L. Scheib, M. Rigo, G. Artioli, A fresh perspective on infrared spectroscopy as a prescreening method for molecular and stable isotopes analyses on ancient human bones, Sci. Rep. 14 (2024) 1028, https://doi.org/10.1038/s41598-024-51518-5.
[27] S. Weiner, O. Bar-Yosef, States of preservation of bones from prehistoric sites in the near east: a survey, J. Archaeol. Sci. 17 (1990) 187–196, https://doi.org/10.1016/0305-4403(90)90058-D.
[28] L.E. Wright, H.P. Schwarcz, Infrared and isotopic evidence for diagenesis of bone apatite at dos Pilas, Guatemala: Palaeodietary implications, J. Archaeol. Sci. 23 (1996) 933–944, https://doi.org/10.1006/jasc.1996.0087.
[29] C.N.G. Trueman, A.K. Behrensmeyer, N. Tuross, S. Weiner, Mineralogical and compositional changes in bones exposed on soil surfaces in Amboseli National Park, Kenya: diagenetic mechanisms and the role of sediment pore fluids, J. Archaeol. Sci. 31 (2004) 721–739, https://doi.org/10.1016/j.jas.2003.11.003.
[30] M. Lebon, I. Reiche, X. Gallet, L. Bellot-Gurlet, A. Zazzo, Rapid quantification of bone collagen content by ATR-FTIR spectroscopy, Radiocarbon 58 (2016) 131–145, https://doi.org/10.1017/RDC.2015.11.
[31] C. Scaggion, G. Dal Sasso, L. Nodari, L. Pagani, N. Carrara, A. Zotti, T. Banzato, D. Usai, L. Pasqualetto, G. Gadioli, G. Artioli, An FTIR-based model for the diagenetic alteration of archaeological bones, J. Archaeol. Sci. 161 (2024) 105900, https://doi.org/10.1016/j.jas.2023.105900.
[32] A. Anzellini, Spectroscopically derived indices for the assessment of natural diagenesis in archaeological bone: a review, Appl. Spectrosc. Rev. 60 (2025) 337–355, https://doi.org/10.1080/05704928.2024.2435292.
[33] M.T. Kirchner, H.G.M. Edwards, D. Lucy, A.M. Pollard, Ancient and modern specimens of human teeth: a Fourier transform Raman spectroscopic study, J. Raman Spectrosc. 28 (1997) 171–178, https://doi.org/10.1002/(SICI)1097-4555(199702)28:2/3%253C171::AID-JRS63%253E3.0.CO;2-V.
[34] W.Al. Sekhaneh, Y.H. Akkam, G. Kamel, A. Drabee, J. Popp, Investigation of ancient teeth using Raman spectroscopy and synchrotron radiation Fourier-transform infrared (SR-μFTIR): mapping and novel method of dating, Dig. J. Nanomater. Bios. 16 (2021), https://doi.org/10.15251/DJNB.2021.162.713.
[35] E. Greco, A.M. Gennaro, D. Piombino-Mascali, D. Costanzo, S. Accardo, S. Licen, P. Barbieri, S. Fornasaro, S. Semeraro, E. Marin, S. Signoretti, C. Gabriele, M. Gaspari, Dental proteomic analyses and Raman spectroscopy for the estimation of the biological sex and age of human remains from the Greek cemetery of san Giorgio extra, Reggio Calabria (Italy), Microchem. J. 195 (2023) 109472, https://doi.org/10.1016/j.microc.2023.109472.
[36] W.J. Pestle, F. Ahmad, B.J. Vesper, G.A. Cordell, M.D. Colvard, Ancient bone collagen assessment by hand-held vibrational spectroscopy, J. Archaeol. Sci. 42 (2014) 381–389, https://doi.org/10.1016/j.jas.2013.11.014.
[37] W.J. Pestle, V. Brennan, R.L. Sierra, E.K. Smith, B.J. Vesper, G.A. Cordell, M. D. Colvard, Hand-held Raman spectroscopy as a pre-screening tool for archaeological bone, J. Archaeol. Sci. 58 (2015) 113–120, https://doi.org/10.1016/j.jas.2015.03.027.
[38] O. Madden, D.M.W. Chan, M. Dundon, C.A.M. France, Quantifying collagen quality in archaeological bone: improving data accuracy with benchtop and handheld Raman spectrometers, J. Archaeol. Sci. Rep. 18 (2018) 596–605, https://doi.org/10.1016/j.jasrep.2017.11.034.
[39] C. Ryder, G. Celis, T. Devièse, S. Talamo, K. Douka, M. Collins, A. Perri, H. Thakar, W. Pestle, M. Sponheimer, Refining near-infrared spectroscopy for collagen quantification: a new predictive model for archaeological bone, J. Archaeol. Sci. 185 (2026) 106448, https://doi.org/10.1016/j.jas.2025.106448.
[40] F. Lugli, G. Sciutto, P. Oliveri, C. Malegori, S. Prati, L. Gatti, S. Silvestrini, M. Romandini, E. Catelli, M. Casale, S. Talamo, P. Iacumin, S. Benazzi, R. Mazzeo, Near-infrared hyperspectral imaging (NIR-HSI) and normalized difference image (NDI) data processing: an advanced method to map collagen in archaeological bones, Talanta 226 (2021) 122126, https://doi.org/10.1016/j.talanta.2021.122126.
[41] N. Hoke, J. Burger, C. Weber, N. Benecke, G. Grupe, M. Harbeck, Estimating the chance of success of archaeometric analyses of bone: UV-induced bone fluorescence compared to histological screening, Palaeogeogr. Palaeoclimatol. Palaeoecol. 310 (2011) 23–31, https://doi.org/10.1016/j.palaeo.2011.03.021.
[42] S. Hillson, Teeth, 2nd ed., Cambridge University Press, 2005 https://doi.org/10.1017/CBO9780511614477.
[43] N. Psonis, C.N. De Carvalho, S. Figueiredo, E. Tabakaki, D. Vassou, N. Poulakakis, D. Kafetzopoulos, Molecular identification and geographic origin of a post-medieval elephant finding from southwestern Portugal using high-throughput sequencing, Sci. Rep. 10 (2020) 19252, https://doi.org/10.1038/s41598-020-75323-y.
[44] N. Psonis, D. Vassou, D. Kafetzopoulos, Testing a series of modifications on genomic library preparation methods for ancient or degraded DNA, Anal. Biochem. 623 (2021) 114193, https://doi.org/10.1016/j.ab.2021.114193.
[45] M.E. Allentoft, M. Sikora, K.-G. Sjögren, S. Rasmussen, M. Rasmussen, J. Stenderup, P.B. Damgaard, H. Schroeder, T. Ahlström, L. Vinner, A.-S. Malaspinas, A. Margaryan, T. Higham, D. Chivall, N. Lynnerup, L. Harvig, J. Baron, P.D. Casa, P. Dąbrowski, P.R. Duffy, A.V. Ebel, A. Epimakhov, K. Frei, M. Furmanek, T. Gralak, A. Gromov, S. Gronkiewicz, G. Grupe, T. Hajdu, R. Jarysz, V. Khartanovich, A. Khokhlov, V. Kiss, J. Kolář, A. Kriiska, I. Lasak, C. Longhi, G. McGlynn, A. Merkevicius, I. Merkyte, M. Metspalu, R. Mkrtchyan, V. Moiseyev, L. Paja, G. Pálfi, D. Pokutta, Ł. Pospieszny, T.D. Price, L. Saag, M. Sablin, N. Shishlina, V. Smrčka, V.I. Soenov, V. Szeverényi, G. Tóth, S.V. Trifanova, L. Varul, M. Vicze, L. Yepiskoposyan, V. Zhitenev, L. Orlando, T. Sicheritz-Pontén, S. Brunak, R. Nielsen, K. Kristiansen, E. Willerslev, Population genomics of bronze age Eurasia, Nature 522 (2015) 167–172, https://doi.org/10.1038/nature14507.
[46] M.-T. Gansauge, T. Gerber, I. Glocke, P. Korlević, L. Lippik, S. Nagel, L.M. Riehl, A. Schmidt, M. Meyer, Single-stranded DNA library preparation from highly degraded DNA using *T4* DNA ligase, Nucleic Acids Res. (2017) gkx033, https://doi.org/10.1093/nar/gkx033.
[47] M.-T. Gansauge, M. Meyer, A method for single-stranded ancient DNA library preparation, in: B. Shapiro, A. Barlow, P.D. Heintzman, M. Hofreiter, J.L. A. Paijmans, A.E.R. Soares (Eds.), Ancient DNA, Springer New York, New York, NY, 2019, pp. 75–83, https://doi.org/10.1007/978-1-4939-9176-1_9.
[48] N. Rohland, I. Glocke, A. Aximu-Petri, M. Meyer, Extraction of highly degraded DNA from ancient bones, teeth and sediments for high-throughput sequencing, Nat. Protoc. 13 (2018) 2447–2461, https://doi.org/10.1038/s41596-018-0050-5.
[49] É. Harney, O. Cheronet, D.M. Fernandes, K. Sirak, M. Mah, R. Bernardos, N. Adamski, N. Broomandkhoshbacht, K. Callan, A.M. Lawson, J. Oppenheimer, K. Stewardson, F. Zalzala, A. Anders, F. Candilio, M. Constantinescu, A. Coppa, I. Ciobanu, J. Dani, Z. Gallina, F. Genchi, E.G. Nagy, T. Hajdu, M. Hellebrandt, A. Horváth, Á. Király, K. Kiss, B. Kolozsi, P. Kovács, K. Köhler, M. Lucci, I. Pap, S. Popovici, P. Raczky, A. Simalcsik, T. Szeniczey, S. Vasilyev, C. Virag, N. Rohland, D. Reich, R. Pinhasi, A minimally destructive protocol for DNA extraction from ancient teeth, Genome Res. 31 (2021) 472–483, https://doi.org/10.1101/gr.267534.120.
[50] S. Neuenschwander, D.I. Cruz Dávalos, L. Anchieri, B. Sousa Da Mota, D. Bozzi, S. Rubinacci, O. Delaneau, S. Rasmussen, A.-S. Malaspinas, Mapache: a flexible pipeline to map ancient DNA, Bioinformatics 39 (2023) btad028, https://doi.org/10.1093/bioinformatics/btad028.
[51] F.A. Shah, Towards refining Raman spectroscopy-based assessment of bone composition, Sci. Rep. 10 (2020) 16662, https://doi.org/10.1038/s41598-020-73559-2.
[52] C.A.M. France, D.B. Thomas, C.R. Doney, O. Madden, FT-Raman spectroscopy as a method for screening collagen diagenesis in bone, J. Archaeol. Sci. 42 (2014) 346–355, https://doi.org/10.1016/j.jas.2013.11.020.
[53] K.A. DeRocher, P.J.M. Smeets, B.H. Goodge, M.J. Zachman, P.V. Balachandran, L. Stegbauer, M.J. Cohen, L.M. Gordon, J.M. Rondinelli, L.F. Kourkoutis, D. Joester, Chemical gradients in human enamel crystallites, Nature 583 (2020) 66–71, https://doi.org/10.1038/s41586-020-2433-3.
[54] K. Sarna-Boś, P. Boguta, K. Skic, D. Wiącek, P. Maksymiuk, J. Sobieszczański, R. Chałas, Physicochemical properties and surface characteristics of ground human teeth, Molecules 27 (2022) 5852, https://doi.org/10.3390/molecules27185852.
[55] S. Alpaslan-Roodenberg, D. Anthony, H. Babiker, E. Bánffy, T. Booth, P. Capone, A. Deshpande-Mukherjee, S. Eisenmann, L. Fehren-Schmitz, M. Frachetti, R. Fujita, C.J. Frieman, Q. Fu, V. Gibbon, W. Haak, M. Hajdinjak, K.P. Hofmann, B. Holguin, T. Inomata, H. Kanzawa-Kiriyama, W. Keegan, J. Kelso, J. Krause, G. Kumaresan, C. Kusimba, S. Kusimba, C. Lalueza-Fox, B. Llamas, S. MacEachern, S. Mallick, H. Matsumura, A.Y. Morales-Arce, G.M. Matuzeviciute, V. Mushrif-Tripathy, N. Nakatsuka, R. Nores, C. Ogola, M. Okumura, N. Patterson, R. Pinhasi, S.P. R. Prasad, M.E. Prendergast, J.L. Punzo, D. Reich, R. Sawafuji, E. Sawchuk, S. Schiffels, J. Sedig, S. Shnaider, K. Sirak, P. Skoglund, V. Slon, M. Snow, M. Soressi, M. Spriggs, P.W. Stockhammer, A. Szécsényi-Nagy, K. Thangaraj, V. Tiesler, R. Tobler, C.-C. Wang, C. Warinner, S. Yasawardene, M. Zahir, Ethics of DNA research on human remains: five globally applicable guidelines, Nature 599 (2021) 41–46, https://doi.org/10.1038/s41586-021-04008-x.